Reversible Redox Chemistry and Catalytic C(sp(3))-H Amination Reactivity of a Paramagnetic Pd Complex Bearing a Redox-Active o-Aminophenol-Derived NNO Pincer Ligand

Broere, D.L.J.; van Leest, N.P.; de Bruin, B.; Siegler, M.A.; van der Vlugt, J.I.

DOI
10.1021/acs.inorgchem.6b01192

Publication date
2016

Document Version
Final published version

Published in
Inorganic Chemistry

Inorganic Chemistry

Article

pubs.acs.org/IC

Reversible Redox Chemistry and Catalytic C(sp^3)–H Amination Reactivity of a Paramagnetic Pd Complex Bearing a Redox-Active *o*-Aminophenol-Derived NNO Pincer Ligand

Daniël L. J. Broere,[†] Nicolaas P. van Leest,[†] Bas de Bruin,[†] Maxime A. Siegler,[‡] and Jarl Ivar van der Vlugt*[,†]

[†]Homogeneous, Supramolecular & Bio-inspired Catalysis, van't Hoff Institute for Molecular Sciences, University of Amsterdam, Science Park 904, 1098 XH Amsterdam, The Netherlands

[‡]Department of Chemistry, John Hopkins University, Baltimore, Maryland 21218, United States

Supporting Information

ABSTRACT: The synthesis, spectroelectrochemical characterization (ultraviolet–visible and nuclear magnetic resonance), solid state structures, and computational metric parameters of three isostructural PdCl(**NNO**) complexes **1** [PdCl(**NNO**^{ISQ})], **2** {[PdCl(**NNO**^{AP})]$^-$}, and **5** {[PdCl(**NNO**^{IBQ})]$^+$} (**NNO** = *o*-aminophenol-derived redox-active ligand with a pendant pyridine) with different **NNO** oxidation states are described. The reduced diamagnetic complex **2** readily reacts with halogenated solvents, including lattice solvent from crystalline pure material, as supported by spectroscopic data and density functional theory calculations. Thorough removal of chlorinated impurities allows for modest catalytic turnover in the conversion of 4-phenylbutyl azide into N-protected 2-phenylpyrrolidine, which is the first example of a palladium-catalyzed radical-type transformation facilitated by a redox-active ligand as well as the first C–H amination mediated by ligand-to-substrate single-electron transfer.

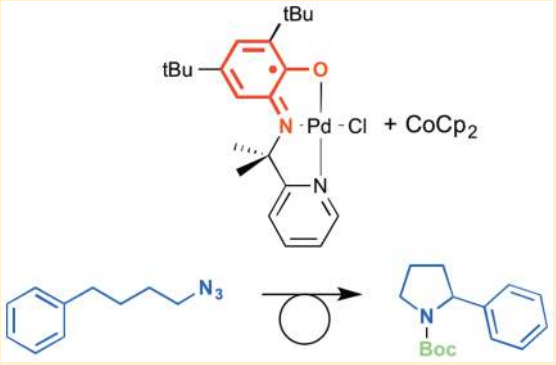

INTRODUCTION

Redox-active ligands are highly relevant for many metalloenzymatic transformations.[1] In synthetic inorganic chemistry, these systems can act as a (multi)electron reservoir, as a reactive ligand, or as a site for radical reactivity when combined with transition metals.[2,3] Various classes of redox-active ligands have been developed and intensely investigated in the past several decades, finding applications in catalysis[4] and materials science.[5] A distinct class consists of the redox-active *o*-aminophenol-derived ligands, which have been studied in great detail by various groups.[6−10] These ligands can coordinate to transition metals in a bisanionic amidophenolato (**NO**^{AP}), a monoanionic iminosemiquinonato (**NO**^{ISQ}), and a neutral iminobenzoquinone oxidation state (**NO**^{IBQ}) (Scheme 1). Analysis of the metric parameters in the **NO** ring obtained from single-crystal X-ray crystallography can provide key information about the oxidation state of the redox-active ligand, as significant dearomatization takes place upon one- and two-electron oxidation of an **NO**^{AP} ligand. On the basis of a comprehensive analysis of structural data, Brown has developed a method that allows for the quantification of the oxidation state for *o*-aminophenol- and *o*-catechol-derived ligands.[11] Using this method, a numerical "metrical oxidation state" (MOS) can be assigned to determine the oxidation state for aminophenol-derived systems with, e.g., d^8 metals.

Single-electron transfer from a limited number of mononuclear metalloradical centers has been exploited to induce selective reduction of substrates, allowing radical-type transformations.[12−16] However, single-electron transfer from a redox-active ligand to a substrate without changing the oxidation state of the accompanying metal is much rarer.[17] This concept may hold promise for imparting radical-type reactivity onto redox-inert main group or "noble" metal centers and thus could potentially expand the scope for substrate coordination and reaction pathways significantly. As a first entry in this emerging field of research, we recently reported intramolecular redox-active ligand-to-substrate single-electron

Scheme 1. Three Possible Oxidation States of *o*-Aminophenol-Derived Ligands

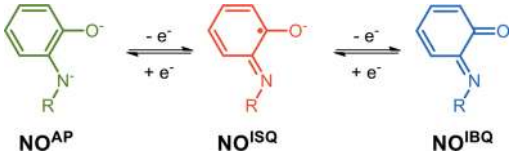

Received: May 15, 2016
Published: August 15, 2016

DOI: 10.1021/acs.inorgchem.6b01192
Inorg. Chem. 2016, 55, 8603–8611

transfer to generate a reactive substrate-centered radical, using complex **1** [PdCl(**NNO**^{ISQ})] as a well-defined starting species.[18] As proof-of-principle reactivity, the intramolecular sp^3 C−H amination of 4-phenylbutyl azide (**3**) using complex **2** (generated by *in situ* reduction of **1** with $CoCp_2$) was demonstrated (Scheme 2), but catalytic turnover to the desired

Scheme 2. Reduction of Paramagnetic 1 To Yield Diamagnetic 2 (top) and Intramolecular sp^3 C−H Amination of 4-Phenylbutyl Azide 3 To Generate Pyrrolidine 4 by Intramolecular Ligand-to-Substrate Single-Electron Transfer on Pd^{II} (bottom)

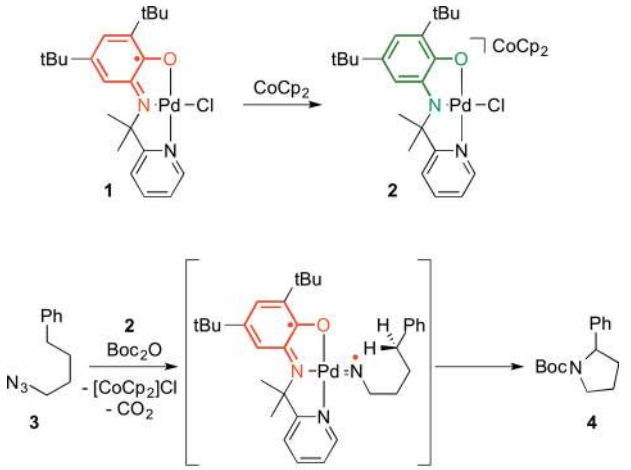

pyrrolidine **4** was not achieved. To identify and circumvent potential bottlenecks for catalytic applications of the combination of this redox-active pincer ligand and Pd(II), we herein detail the coordination chemistry and reactivity of the Pd(**NNO**) complexes in all three ligand oxidation states (Scheme 1). Furthermore, we describe halogen atom abstraction reactivity as a potential deactivation pathway and a strategy for invoking modest catalytic turnover in the conversion of azide **3** to pyrrolidine **4**. This results in the first catalytic example of a radical-type transformation in the coordination sphere of Pd^{II} facilitated by a redox-active ligand.

RESULTS AND DISCUSSION

Structural Comparison of Pd(NNO) Species 1, 2, and 5 with Different NNO Oxidation States. We previously reported the straightforward synthesis of brown paramagnetic square planar complex **1**, Pd^{II}Cl(**NNO**^{ISQ}), which crystallized from chloroform with 1 equiv of lattice solvent per Pd complex.[18] A combination of cyclic and differential pulse voltammetry showed a fully reversible one-electron oxidation ($E^{1/2}_{ox}$) at 0.10 V versus Fc/Fc$^+$ and a one-electron reduction event ($E^{1/2}_{red}$) at −0.96 V versus Fc/Fc$^+$ of **1** in a CH_2Cl_2 solution.[19] Chemical reduction using cobaltocene was shown to be facile, resulting in purple crystalline diamagnetic complex **2**, [$CoCp_2$][Pd^{II}Cl(**NNO**^{AP})].[18]

Chemical oxidation of **1** to **5** (Scheme 3) proceeded equally smoothly with several oxidants, including Ag^I salts and thianthrenium tetrafluoroborate. An equimolar reaction of **1** with acetylferrocenium tetrafluoroborate allowed for the isolation of [Pd^{II}Cl(**NNO**^{IBQ})]BF_4 (**5**) as a red solid in good yield. Notably, the resonances in the ^{1}H NMR spectrum of isolated **5** were significantly broadened in several solvents

Scheme 3. Synthesis of the One-Electron-Reduced and One-Electron-Oxidized Species 2 and 5, Respectively[a]

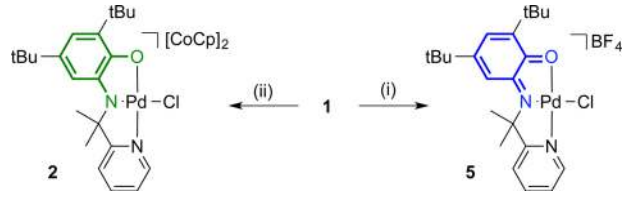

[a]Reagents and conditions: (i) $CoCp_2$, C_6H_6, room temperature; (ii) acetylferrocenium tetrafluoroborate, C_6H_6, room temperature.

(CD_2Cl_2, CD_3CN, and $CDCl_3$), especially for the two protons on the redox-active **NO** ring. In contrast, when the oxidation was performed in CD_3CN with a small excess of SelectFluor, which is a strong oxidant, only sharp signals were observed (see the Supporting Information). The protons on the redox-active **NO** ring appear as two well-separated singlets at 7.43 and 6.74 ppm in CD_3CN and are clearly separated from all pyridine protons. Vapor diffusion of diethyl ether into this mixture resulted in red single crystals of **5** and colorless crystals of the one-electron-reduced organic byproduct, which could be separated by hand. However, the ^{1}H NMR spectrum of the redissolved red crystals again showed broadened resonances.[20]

The structure for **5** was confirmed by X-ray structure determination. This allowed a direct comparison of the metric parameters of the redox series of **1**, **2**, and **5**. The overall geometries of the anionic Pd-containing fragment of complex **2** (Figure 1, left) and the cationic Pd fragment of **5** (right) are almost isostructural to that of the distorted square planar **1** (center). However, the metric parameters for the **NO** ring in **2**, which were reproduced by density functional theory (DFT) calculations (b3-lyp, def2-TZVP), confirm the amidophenolate (**AP**) oxidation state (MOS = −1.76 ± 0.17).[11] The unit cell displays short contacts between hydrogen atoms of cationic cobaltocenium ions and C and O atoms of the amidophenolate, suggestive of partial negative charges on the **NO** ring. Likewise, the metric parameters for the **NO** ring in **5** are characteristic of the iminobenzoquinone (**IBQ**) ligand oxidation state (MOS = −0.17 ± 0.05).[11] The unit cell shows a disordered tetrafluoroborate anion with short contacts (<2.7 Å) to both C1 and C6 of two separate **NNO**^{IBQ} ligands, indicative of partial positive charges in the **NO** ring. Wieghardt et al. observed similar close contacts between BF_4 anions and (di)cationic Pd(**NO**^{IBQ}) species.[21]

With the series in hand, some clear trends in metric parameters can be observed. Going from the **NNO**^{AP} to the **NNO**^{IBQ} ligand oxidation states, we observed a clear elongation of the C1−C2, C3−C4, and C5−C6 bonds of the **NO** ring, whereas bonds C2−C3, C4−C5, C1−O1, and C6−N1 are significantly shortened. These trends nicely fit with the resonance structures in Scheme 1.[22] Another clear trend is the shortening of the Pd1−Cl and Pd1−N2 bonds going from the **NNO**^{AP} to the **NNO**^{IBQ} ligand oxidation state, reflecting the more electron-deficient nature of the metal center due to a decreased level of electron donation from the **NO** ring. The increased extent of pyramidalization of N1 upon reduction from the **NNO**^{IBQ} to the **NNO**^{AP} ligand oxidation state is ascribed to an increase in the sp^3 character of N1 (Figure 1). The Pd1−O1 and Pd1−N1 bond lengths do not vary strongly in the redox series, which may reflect a balance between geometric factors (planar orientation of N1 in **5** vs slightly

DOI: 10.1021/acs.inorgchem.6b01192
Inorg. Chem. 2016, 55, 8603−8611

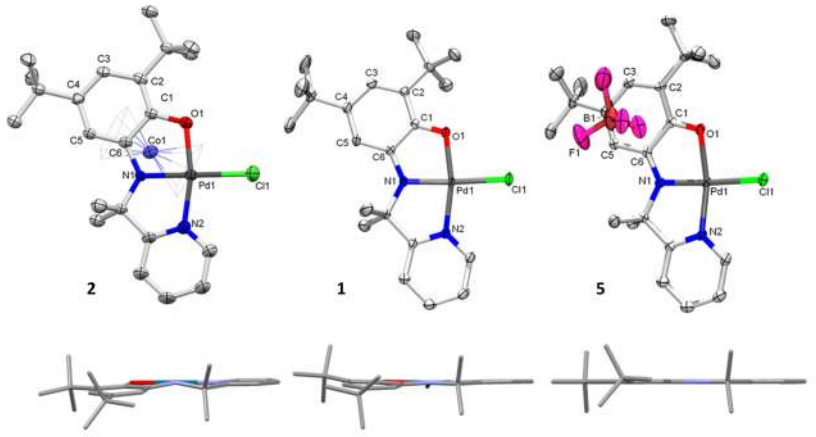

Bond	XRD	DFT	XRD	DFT	XRD	DFT
C1-C2	1.396(6)	1.398	1.423(4)	1.425	1.443(4)	1.447
C2-C3	1.413(7)	1.402	1.377(3)	1.373	1.343(5)	1.355
C3-C4	1.397(8)	1.388	1.426(3)	1.420	1.456(5)	1.456
C4-C5	1.405(6)	1.402	1.370(3)	1.375	1.343(4)	1.359
C5-C6	1.395(9)	1.403	1.420(3)	1.422	1.434(4)	1.432
C6-C1	1.450(8)	1.434	1.452(3)	1.425	1.500(4)	1.506
C1-O1	1.354(7)	1.335	1.310(2)	1.296	1.254(4)	1.251
C6-N1	1.380(8)	1.380	1.351(2)	1.348	1.304(4)	1.311
Pd1-N1	1.933(6)	1.961	1.9281(17)	1.996	1.945(3)	1.973
Pd1-O1	2.004(4)	1.995	1.9923(14)	2.020	2.028(2)	2.056
Pd1-N2	2.001(5)	2.023	1.9975(17)	2.017	1.969(2)	2.000
Pd1-Cl	2.3514(16)	2.394	2.3113(6)	2.320	2.2785(9)	2.264
MOS	-1.76 ± 0.17	-1.66 ± 0.12	-1.00 ± 0.05	-0.93 ± 0.06	-0.17 ± 0.05	-0.17 ± 0.04

Figure 1. Displacement ellipsoid plots (50% probability level) (top) of complexes **2** (left), **1** (center), and **5** (right). Below each ellipsoid plot is a view through the N1−Pd1 bond showing the increasing sp^3 character of the **NO** nitrogen on going from the most oxidized to the most reduced ligand oxidation state. Hydrogen atoms, disorder, and solvent molecules have been omitted for the sake of clarity. Table containing relevant experimental (XRD) and computed (DFT) metric parameters and MOS values of the three structures.

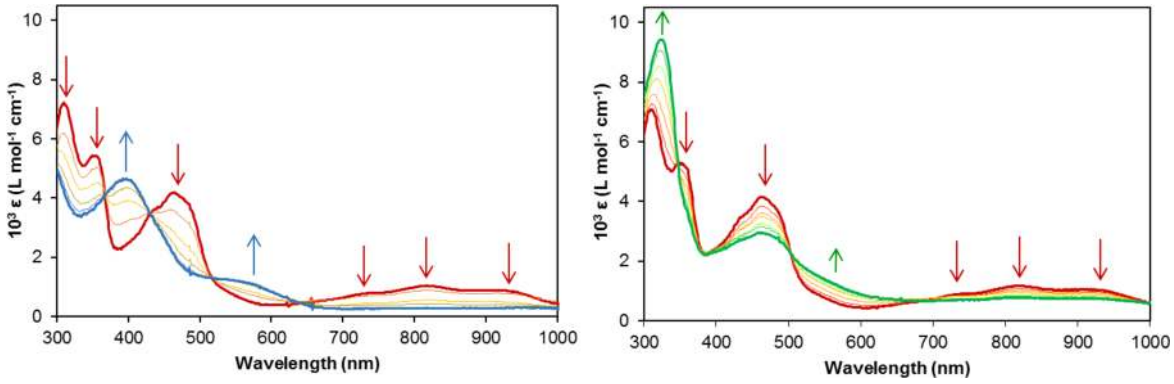

Figure 2. Stacked UV−vis spectra of the one-electron oxidation of **1** to **5** (left) and the one-electron reduction of **1** to **2** (right) by cumulative addition of aliquots (0.2 equiv) of SelectFluor and $CoCp_2$, respectively.

pyramidalized N1 in **2**) and electronic factors (more covalent bonding character in **2**). Very recently, Mukherjee et al. also reported isostructural Pd^{II} complexes with an aminophenol-derived redox-active tetradentate ligand in all three ligand oxidation states, showing similar trends.[23]

Ultraviolet−Visible (UV−vis) Spectra of Pd(NNO) Complexes 1, 2, and 5. To characterize the spectral features of the **NNO** ligand in its three oxidation states, we performed UV−vis titrations of the one-electron oxidation and one-electron reduction of complex **1** in MeCN to generate **5** and **2**, respectively (Figure 2). For the ligand-centered one-electron oxidation of **1**, aliquots containing 0.2 equiv of SelectFluor were added, resulting in clear conversion to **5** (Figure 2, left) after the addition of 1.0 equiv. Four isosbestic points are present (at λ = 371, 428, 513, and 636 nm), and no additional spectral changes were visible (in UV−vis or ^{19}F NMR) upon addition of more SelectFluor, confirming that the latter functions as a one-electron oxidant and that no secondary reactions occur. The

DOI: 10.1021/acs.inorgchem.6b01192
Inorg. Chem. 2016, 55, 8603−8611

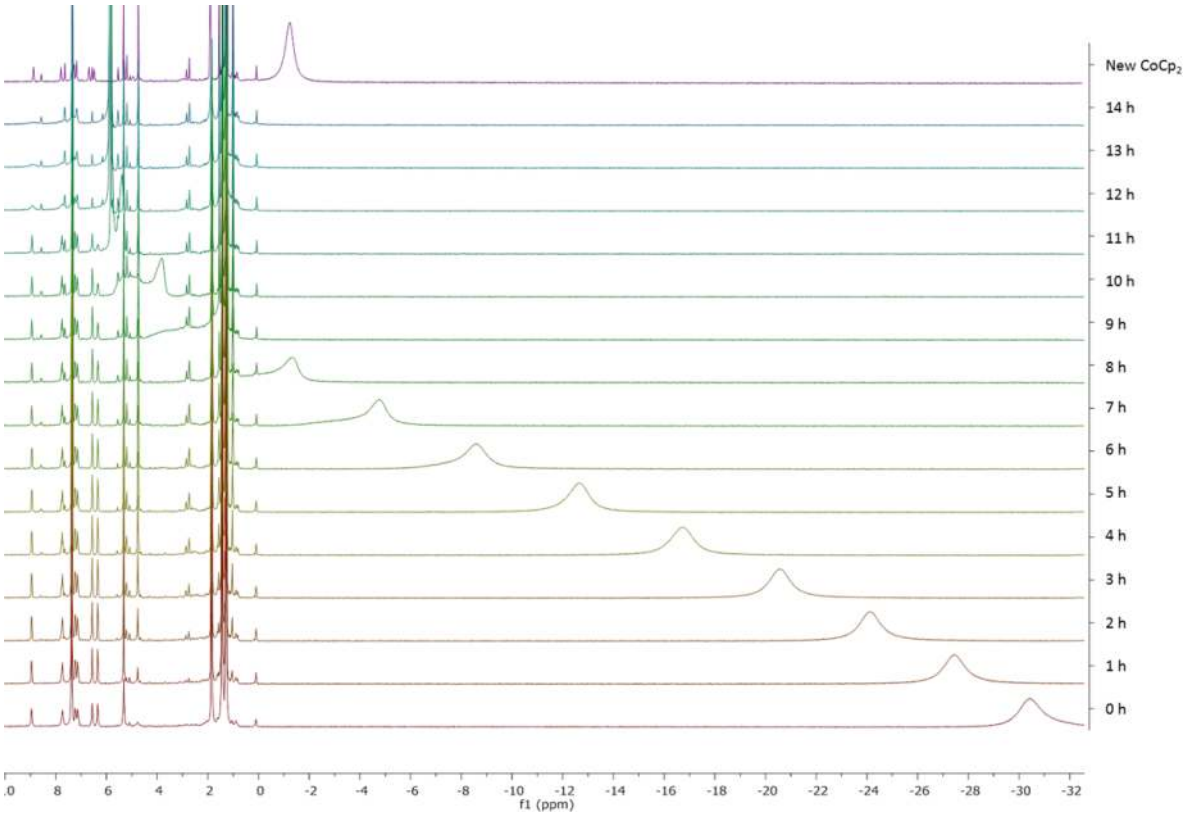

Figure 3. Stacked ^{1}H NMR spectra of a CD_2Cl_2 solution of **1** in the time range of 0−14 h after the addition of 3 equiv of $CoCp_2$ and addition of new $CoCp_2$ (top spectrum).

intraligand charge-transfer bands at λ = 730, 815, and 918 nm, characteristic for the $\mathbf{NO}^{\mathbf{ISQ}}$ fragment,[6d,24] completely disappear upon oxidation, which is in agreement with generation of the $\mathbf{NO}^{\mathbf{IBQ}}$ derivative. Additionally, new bands at λ = 401 and 550 nm appear that may be attributed to an $\mathbf{NO}^{\mathbf{IBQ}}$ fragment.[17b,18b,21,23]

For the one-electron reduction of **1**, aliquots containing 0.2 equiv of $CoCp_2$ were added until clear conversion to **2** (Figure 2, right) was observed after 1.2 equiv. The small excess required is ascribed to partial oxidation by traces of O_2 as a result of the highly sensitive nature of complex **2**. Isosbestic points were found at λ = 348, 389, 505, and 698 nm, and no spectral changes beyond 400 nm were observed after the addition of more $CoCp_2$ (Figure 2, right). Similar to the one-electron oxidation to **5** and the recently reported PNO analogue,[17b] bleaching of the $\mathbf{NO}^{\mathbf{ISQ}}$ intraligand charge-transfer bands is in agreement with ligand-centered reduction to the $\mathbf{NNO}^{\mathbf{AP}}$ ligand oxidation state. Two additional disappearing bands (λ = 430 and 469 nm) are attributed to metal-to-ligand charge transfer (MLCT) to the electron-deficient $\mathbf{NO}^{\mathbf{ISQ}}$ ring, similar to that seen for the system reported by Mukherjee et al.[23] The red-shifted, high-intensity band at λ = 305 nm is ascribed to the presence of $[CoCp_2]^+$.[25]

NMR Spectroscopic Investigations of the Stability of Complex 2 in Chlorinated Solvents. Paramagnetic complex **1** is bench-stable as a solid and soluble in dichloromethane and related halogenated solvents, with no sign of decomposition after prolonged standing. Addition of a slight excess (1.2 equiv) of $CoCp_2$ to a solution of **1** in CD_3CN allowed for assignment and direct comparison of all ^{1}H NMR resonances of the reduced species **2** with the data obtained for **5**. The two protons on the amidophenolate ring appear at 6.48 and 6.24 ppm for **2**. The smaller separation between the two signals compared to that in the data obtained for **5** reflects the aromatic character of the **NO** ring in **2**. Reaction of **1** with $CoCp_2$ in CD_2Cl_2 results in clean formation of **2**, with identical initial NMR signatures as observed in CD_3CN, but the spectral features dramatically changed over time in dichloromethane. The cobaltocenium protons initially appeared as a strongly broadened and upfield-shifted signal that sharpened and moved downfield over time (Figure 3). Correspondingly, the initially observed signals for **2** broadened and eventually disappeared. Re-addition of $CoCp_2$ regenerated the spectral features of **2** and shifted the $[CoCp_2]^+$ upfield. These observations suggest that **2** undergoes a follow-up reaction in CD_2Cl_2 to (re)generate **1**. Starting from an equimolar mixture of the two compounds at 298 K results in a 1.4×10^3:1 **2**:**1** ratio [K_{eq} of 1.8×10^6 (see the Supporting Information)], based on the relative redox potentials of $CoCp_2$ and **1**. Thus, reduction of **1** with $CoCp_2$ provides an almost quantitative conversion to **2**. The slight excess of $CoCp_2$ is in electrochemical self-exchange with $[CoCp_2]^+$ cations in solution, causing an upfield shift and broadening of the $[CoCp_2]^+$ resonance.[26] The $[CoCp_2]^+$ resonance slowly moving downfield upon reduction of **1** to **2** shows that the $CoCp_2$ concentration decreases over time. Abstraction of a chlorine atom from the solvent upon chloride dissociation from **2** to regenerate **1** and $[CoCp_2]Cl$ would account for gradual disappearance of the $[Pd(\mathbf{NNO}^{\mathbf{AP}})]^-$ resonances and reappearance upon addition of additional $CoCp_2$ (Scheme 4). Performing the reduction in CD_3CN with $CHCl_3$, 1 equiv present as lattice solvent in crystalline **1** per Pd complex, and an excess of $CoCp_2$ led to the gradual disappearance of the ^{1}H NMR resonance of chloroform. Addition of PPh_3 to **2** in CH_2Cl_2 generated the neutral complex

DOI: 10.1021/acs.inorgchem.6b01192
Inorg. Chem. 2016, 55, 8603−8611

Scheme 4. Redox Equilibrium of 1 and $CoCp_2$ with 2 and the Reactivity of 2 toward CH_2Cl_2 and PPh_3 To Form 1 and $[CoCp_2]Cl$ and $PdPPh_3(NNO^{AP})$, Respectively

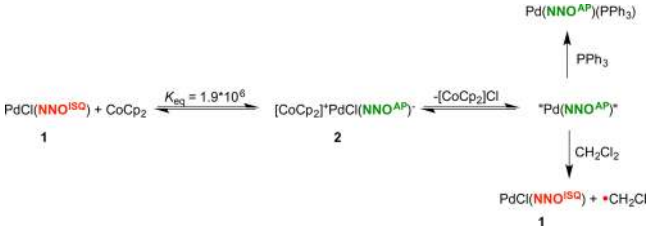

$Pd(\mathbf{NNO^{AP}})$ (PPh_3) and halted the shifting of the $[CoCp_2]^+$ resonance, as reaction of **2** with solvent is prevented. Partial decomposition into an unidentified species can also be observed in the NMR spectra depicted in Figure 3. Cold-spray ESI-MS analysis of the resulting mixture showed *m*/*z* values corresponding to **NNO**-containing species (with and without Pd) with added CH_2Cl fragments, suggestive of the formation of chloromethyl radicals and subsequent reaction with the organic ligand.[27]

DFT Calculations. To understand the reactivity of **2** with CH_2Cl_2, we performed DFT calculations (b3-lyp, def2-TZVP) on potential intermediates generated by homolytic C−Cl cleavage, based on the NMR spectroscopic observation that **1** is regenerated after reduction with $CoCp_2$ in the presence of CH_2Cl_2 (or $CHCl_3$).[28] We have included the COSMO solvation model with the dielectric constant of CH_2Cl_2 (ε = 8.9). The energy profile in Figure 4 involves the following

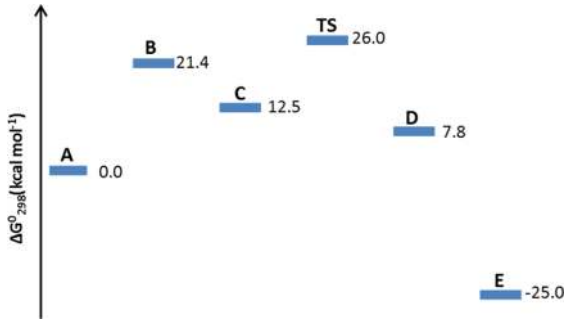

Figure 4. DFT-calculated free energy profile (ΔG°_{298}) using the COSMO solvation model for the homolytic cleavage of the Cl−CH_2Cl bond (b3-lyp, def2-TZVP).

intermediates: (**A**) $[PdCl(\mathbf{NNO^{AP}})]^-$ + CH_2Cl_2, (**B**) $Pd(\mathbf{NNO^{AP}})$ + CH_2Cl_2 + Cl^-, (**C**) $Pd(\mathbf{NNO^{AP}})(CH_2Cl_2)$ + Cl^-, (**TS**) $Pd(\mathbf{NNO^{AP}})$ $(Cl^{\bullet}\cdots{}^{\bullet}CH_2Cl)$ + Cl^-, (**D**) $PdCl(\mathbf{NNO^{ISQ}})$ + $^{\bullet}CH_2Cl$ + Cl^-, and (**E**) $PdCl(\mathbf{NNO^{ISQ}})$ + $ClCH_2CH_2Cl$ + Cl^-. Dissociation of chloride from $[PdCl(\mathbf{NNO^{AP}})]^-$ is endergonic by 21.4 kcal mol^{-1}. Subsequent coordination of CH_2Cl_2 to the "naked" neutral $Pd(\mathbf{NNO^{AP}})$ fragment (**A**) is exergonic by −8.9 kcal mol^{-1}.[29] Both a closed-shell singlet (CSS) and triplet solution were found for $Pd(CH_2Cl_2)$-$(\mathbf{NNO^{AP}})$ (**C**), with the CSS being lower in energy by 5.7 kcal mol^{-1}. The barrier (ΔG°_{298}) on the open-shell singlet (OSS) surface for homolytic cleavage of the Cl−CH_2Cl bond relative to species **C** was found to be only 13.5 kcal mol^{-1} (**TS**).[30] The reaction to form $PdCl(\mathbf{NNO^{ISQ}})$ and a short-lived chloromethyl radical ($^{\bullet}CH_2Cl$)[31] is exergonic (ΔG°_{298} = −18.2 kcal mol^{-1}) (**D**). Although we have not detected dichloroethane from chloromethyl radical dimerization (*vide supra*) under the current experimental conditions, this reaction to generate state **E** makes the overall reaction exergonic by −25.0 kcal mol^{-1}, with the rate-determining step (highest barrier) being initial chloride dissociation. It can be suggested that other coupling reactions with this reactive $^{\bullet}CH_2Cl$ intermediate may result in similar energy profiles. The initial chloride dissociation was poorly described (highly endergonic) by calculations in the gas phase (see the Supporting Information), increasing the relative energies of **B**−**E**. As expected, the COSMO solvation model significantly decreased the barrier for this initial step. However, these calculations do not include the cobaltocenium ion. Ion pairing of the chloride anion will undoubtedly result in further stabilization of this fragment. As a result, it is reasonable to assume that this in turn would lower the energies for **B**−**E** even further.

As the DFT calculations indicate facile Cl−CH_2Cl bond cleavage upon coordination of CH_2Cl_2 to the reduced $Pd(\mathbf{NNO^{AP}})$ fragment, we decided to look more closely into this homolytic bond cleavage. Notably, solely a transition state was found on the open-shell singlet (OSS) surface. No transition state could be found on the CSS (involves localized charges) or triplet surface (spin-forbidden reaction). The HOMO of $Pd(CH_2Cl_2)(\mathbf{NNO^{AP}})$ consists of two paired electrons located on the redox-active *o*-amidophenolate fragment. Interestingly, upon homolytic bond cleavage, an intramolecular single-electron transfer from the $\mathbf{NNO^{AP}}$ ligand to the coordinated Cl−CH_2Cl fragment can be observed computationally. The spin density plot of the transition state for homolytic bond cleavage nicely illustrates the generation of an $\mathbf{NNO^{ISQ}}$ ligand radical and a chloromethyl radical (Figure 5).

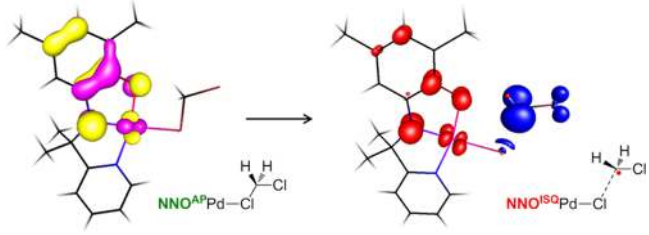

Figure 5. DFT (b3-lyp, def2-TZVP)-calculated HOMO plot for $Pd(CH_2Cl_2)(\mathbf{NNO^{AP}})$ (left) and spin density plot for the transition state of homolytic cleavage of the Cl−CH_2Cl bond on the OSS surface (right).

Having established that complex **2** reacts with chlorinated reagents and given the fact that complex **1** contains $CHCl_3$ in the crystal lattice, we decided to reinvestigate the previously stoichiometric intramolecular radical-type sp^3 C−H amination of azide **3** toward pyrrolidine **4** (Scheme 5). As reported for other systems, di(*tert*-butyl) carbonate (Boc_2O) is added as an *in situ* N-protecting group to avoid catalyst deactivation by

Scheme 5. Conversion of Azide 3 to Boc-Protected Pyrrolidine 4, Linear Boc-Protected Amine 6, and Nitrile 7[a]

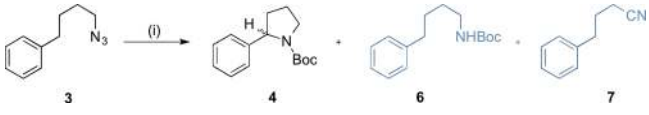

[a]Reagents and conditions: (i) **1** (0.1 equiv), $CoCp_2$ (0.1 equiv), Boc_2O (1 equiv), C_6H_6, 100 °C.

DOI: 10.1021/acs.inorgchem.6b01192
Inorg. Chem. 2016, 55, 8603−8611

product inhibition.[12] Gratifyingly, thorough removal of all $CHCl_3$ lattice solvent in crystalline **1** by freeze-drying from benzene resulted in 2.8 turnovers for the conversion of **3** to **4** after 70 h at 100 °C in benzene in the presence of 1 molar equivalent of cobaltocene ($CoCp_2$) as a reductant to generate **2** *in situ*. Analysis of the product distribution over time showed that pyrrolidine **4** (major product) and amine **6** (minor product) are predominantly formed in the first hours of the reaction (Figure 6). As the formation of these products slows,

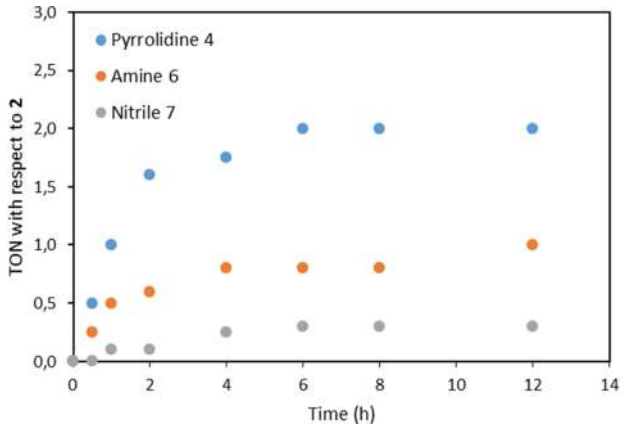

Figure 6. Monitoring of the product distribution for **4**, **6**, and **7** over time during the conversion of **3** (average of two runs).

some (previously unidentified) nitrile **7** is produced.[32] The use of additional equivalents of $CoCp_2$ did not increase the rate of turnover. Attempts to increase the rate of catalytic turnover by changing the reaction temperature, solvent, reagent stoichiometry, or the addition of additives were unsuccessful. Higher temperatures likely induce faster catalyst decomposition, while organoazide activation is inhibited at lower temperatures. Other amine protecting groups (FmocCl, CBzCl, and Ac_2O) gave no conversion. For example, addition of FmocCl generated an undefined orange species, supposedly because of fast reaction with complex **2**. This suggests that, although the Pd(**NNO**) system is catalytically competent in the absence of chlorinated solvent, other deactivation pathways are still operative, limiting the overall turnover for this system. We are currently investigating this in more detail.

CONCLUSIONS

In summary, we have successfully prepared and characterized isostructural Pd complexes containing a redox-active NNO ligand in all three ligand oxidation states. The reduced complex **2** reacts with chlorinated reagents, which leads to deactivation in the intramolecular radical-type sp^3 C–H amination of 4-phenylbutyl azide **3** toward pyrrolidine **4**. A possible mechanism studied by DFT calculations is chlorine atom abstraction via intramolecular single-electron transfer from the redox-active ligand to a coordinated solvent molecule. The presence of only 1 molar equivalent of $CHCl_3$ (as lattice solvent) in the reaction mixture suffices to limit **2** to stoichiometric reactivity in C–H amination. In the absence of chlorinated reagents, (limited) catalytic turnover to **4** was achieved. This is the first catalytic example of a radical-type reaction in the coordination sphere of palladium(II) facilitated by single-electron transfer from a redox-active ligand. We are currently investigating other catalytic reactions with this platform as well as with other transition metals. We are also exploring productive (electrochemical) pathways involving C–X bond activation.[33]

EXPERIMENTAL SECTION

General Methods. All reactions were conducted under an atmosphere of dry dinitrogen or argon using standard Schlenk techniques unless noted otherwise. Compounds **1**–**3** were prepared as previously reported.[18] Acetylferrocenium was prepared according to the literature procedure.[34] All other reagents were purchased from commercial suppliers and used without further purification. THF, benzene, pentane, hexane, and diethyl ether were distilled from sodium benzophenone ketyl. CH_2Cl_2 and methanol were distilled from CaH_2, and toluene was distilled from sodium under nitrogen. NMR spectra were recorded on a Bruker DRX 500, Bruker AMX 400, Bruker DRX 300, or Varian Mercury 300 spectrometer at 298 K unless noted otherwise. Cyclic voltammetry measurements were performed in CH_2Cl_2 (1×10^{-3} M) containing $N(n\text{-}Bu)_4PF_6$ (0.1 M) at room temperature under a N_2 atmosphere using a Pt electrode. All redox potentials are referenced to Fc/Fc^+.

Complex 5 {[PdCl(NNO^{IBQ})]BF_4}. A solution of **1** (24 mg, 0.05 mmol) in benzene (4 mL) was added to a suspension of acetylferrocenium tetrafluoroborate (15 mg, 0.05 mmol) in benzene (1 mL). The mixture was stirred for 2 h after which the precipitate was collected by filtration. The dark red precipitate was washed with benzene (1 mL) and dried *in vacuo*, affording complex **5** as a red solid (21 mg, 78%). ^1H NMR (300 MHz, CD_3CN) (obtained from *in situ* oxidation with SelectFluor): δ 8.70 (d, J = 5.2 Hz, 1H, Py-*H*), 8.21 (ddd, J = 8.6, 7.9, 1.6 Hz, 1H, Py-*H*), 7.56 (m, 2H, Py-*H*), 7.43 (s, 1H, ap-*H*), 6.74 (s, 1H, ap-*H*), 2.09 (s, 6H, *gem*-Me), 1.29 (s, 9H, tBu), 1.27 (s, 9H, tBu). ^{19}F NMR (282 MHz, CD_3CN): δ −151.80 (s). MS-ESI$^+$ (m/z) calcd for $C_{22}H_{30}ClN_2OPd$: 479.108, found 478.965. Anal. Calcd for $C_{22}H_{30}BClF_4N_2OPd$: C, 46.59; H, 5.33; N, 4.94. Found: C, 46.63; H, 5.31; N, 4.89.

General Procedure for an Intramolecular sp^3 C–H Amination Experiment. In a nitrogen-filled glovebox, **1** (2.9 mg, 0.006 mmol, 0.1 equiv), (4-azidobutyl)benzene (10.5 mg, 0.060 mmol, 1.0 equiv), and Boc_2O (13.1 mg, 0.060 mmol, 1.0 equiv) were dissolved in benzene (3.0 mL) and placed in a 25 mL pressure tube. A solution of $CoCp_2$ (1.2 mg, 0.006 mmol, 0.1 equiv) in benzene (2.0 mL) was added to the brown solution, resulting in immediate formation of a bright purple solution. The pressure tube was tightly sealed and heated to 100 °C outside the glovebox. After 24 h, the mixture was cooled to ambient temperature and filtered. 1,3,5-Trimethoxybenzene was added as an internal standard. All volatiles were evaporated by rotary evaporation, and the residue was analyzed by ^1H NMR spectroscopy. When multiple reactions were performed to monitor the reaction at various time intervals, all reaction vessels were prepared under identical conditions in the glovebox and chemicals were taken from stock solutions.

Isolation of Side Product 7. The previously unidentified side product **7** was isolated from the crude reaction mixture by column chromatography (silica plug, DCM, $R_f \approx 0.5$) and characterized as 4-phenylbutyronitrile. Analytic data for this compound are in agreement with literature data.[35]

General Procedure for Following the Formation and Deactivation of [PdCl(NNO^{AP})]$^-$ over Time. In a glovebox, **1** (9.6 mg, 0.02 mmol, 1.0 equiv) was dissolved in CD_2Cl_2 (0.3 mL). To this brown solution was added $CoCp_2$ (11.4 mg, 0.6 mmol, 3.0 equiv) in CD_2Cl_2 (0.3 mL). The bright purple solution was transferred to a J Young NMR tube. ^1H NMR spectra were recorded at regular time intervals. After a few hours, a black precipitate was observed and the solution turned more brownish. To add new $CoCp_2$, the NMR tube was returned to the glovebox and a small amount $CoCp_2$ (approximately 3 mg) was added.

Single-Crystal X-ray Crystallography. *Complex 5.* $C_{22}H_{30}BClF_4N_2OPd$, fw = 567.14, brown plate, 0.61 mm × 0.14 mm × 0.08 mm, triclinic, $P\bar{1}$ (No. 2), a = 7.3768(4) Å, b = 12.0798(7) Å, c = 15.1667(9) Å, α = 93.531(3)°, β = 89.979(4)°, γ = 107.760(3)°, V = 1284.41(13) Å^3, Z = 2, D_x = 1.466 g/cm^3, μ = 0.871 mm^{-1}; 31066

DOI: 10.1021/acs.inorgchem.6b01192
Inorg. Chem. 2016, 55, 8603–8611

reflections were measured on a Bruker D8 Quest Eco diffractometer equipped with a Triumph monochromator (λ = 0.71073 Å) and a CMOS Photon 50 detector at a temperature of 150(2) K up to a resolution of $(\sin\theta/\lambda)_{max}$ = 0.60 Å^{-1}. Intensity data were integrated with the Bruker APEX2 software.[36] Multiscan absorption correction and scaling were performed with SADABS;[37] 4607 reflections were unique (R_{int} = 0.0874), of which 3779 were observed [$I > 2\sigma(I)$]. The structures were determined using intrinsic phasing with SHELXT.[36] Least-squares refinement was performed with SHELXL-2013[38] against F^2 of all reflections. Non-hydrogen atoms were refined freely with anisotropic displacement parameters. The H atoms were placed at calculated positions using the instructions of AFIX 13, AFIX 43, or AFIX 137 with isotropic displacement parameters having values 1.2 or 1.5 times the U_{eq} of the attached C atoms; 470 parameters were refined with 866 restraints. R1/wR2 [$I > 2\sigma(I)$]: 0.0339/0.0628. R1/wR2 (all reflections): 0.0518/0.0679. S = 0.970. Residual electron density between −0.40 and 0.49 e/Å^3. CCDC entry 1477970. The crystal lattice also includes some amount of very disordered lattice solvent molecules. Their contribution was removed in the final refinement using the SQUEEZE procedure in Platon.[39]

Computational Details. Geometry optimizations were conducted using Turbomole[40] coupled with the PQS Baker Optimizer[41] via the BOpt package[42] at the DFT level using the BP86 or b3-lyp functional and the def2-TZVP basis set. The corrected broken symmetry energies ε_{BS} of the open-shell singlets (S = 0) were estimated from energy ε_S of the optimized single-determinant broken symmetry solution and energy ε_{S+1} from a separate unrestricted triplet calculation at the same level, using the approximate correction formula:[43]

$$\varepsilon_{BS} \approx \frac{S_{S+1}{}^2\varepsilon_S - S_S{}^2\varepsilon_{S+1}}{S_{S+1}{}^2 - S_S{}^2}$$

The *tert*-butyl groups on the NNO ligand were replaced with Me groups to decrease the computational time. Energies including the COSMO solvation model were obtained by performing single-point calculations on the b3-lyp, def2-TZVP optimized geometries. Estimated condensed phase (1 L mol^{-1}) free energies and enthalpies were obtained from these data by neglecting the enthalpy RT term and subsequent correction for the condensed phase reference volume [$S_{CP} = S_{GP} + R \times \ln(1/24.5)$]. For the reactions involving reaction with the solvent, a correction of −8 kcal mol^{-1} was made for the condensed phase energies as the there is no entropic penalty for bringing the molecules together.

■ ASSOCIATED CONTENT

Supporting Information

The Supporting Information is available free of charge on the ACS Publications website at DOI: 10.1021/acs.inorgchem.6b01192.

Details for the redox reaction between **1** and $CoCp_2$, NMR spectra, and DFT calculations (PDF)
Crystallographic data (CIF)

■ AUTHOR INFORMATION

Corresponding Author

*E-mail: j.i.vandervlugt@uva.nl.

Notes

The authors declare no competing financial interest.

■ ACKNOWLEDGMENTS

This research was supported by the European Research Council through an ERC Starting Grant (Grant Agreement 279097, *EuReCat*) to J.I.v.d.V. We thank Prof. Joost Reek for discussions and interest in our work. This research is part of the University of Amsterdam Research Priority Area Sustainable Chemistry.

■ REFERENCES

(1) (a) Stubbe, J.; van der Donk, W. A. *Chem. Rev.* **1998**, *98*, 705−762. (b) Harris, D. L. *Curr. Opin. Chem. Biol.* **2001**, *5*, 724−735. (c) Que, L.; Tolman, W. B. *Nature* **2008**, *455*, 333−340. (d) Kaim, W.; Schwederski, B. *Coord. Chem. Rev.* **2010**, *254*, 1580−1588.

(2) Reviews and highlights: (a) Broere, D. L. J.; Plessius, R.; van der Vlugt, J. I. *Chem. Soc. Rev.* **2015**, *44*, 6886−6915. (b) Luca, O. R.; Crabtree, R. H. *Chem. Soc. Rev.* **2013**, *42*, 1440−1459. (c) Munha, R. F.; Zarkesh, R. A.; Heyduk, A. F. *Dalton Trans.* **2013**, *42*, 3751−3766. (d) Praneeth, V. K. K.; Ringenberg, M. R.; Ward, T. R. *Angew. Chem., Int. Ed.* **2012**, *51*, 10228−10234. (e) van der Vlugt, J. I. *Eur. J. Inorg. Chem.* **2012**, *2012*, 363−375. (f) Lyaskovskyy, V.; de Bruin, B. *ACS Catal.* **2012**, *2*, 270−279. (g) Dzik, W. I.; Zhang, X. P.; de Bruin, B. *Inorg. Chem.* **2011**, *50*, 9896−9903. (h) Kaim, W. *Inorg. Chem.* **2011**, *50*, 9752−9765. (i) Dzik, W. I.; van der Vlugt, J. I.; Reek, J. N. H.; de Bruin, B. *Angew. Chem., Int. Ed.* **2011**, *50*, 3356−3358. (j) Dzik, W. I.; de Bruin, B. *Specialist Periodical Report Organometallic Chemistry* **2011**, *37*, 46−78.

(3) Recent examples: (a) Bagh, B.; Broere, D. L. J.; Siegler, M. A.; van der Vlugt, J. I. *Angew. Chem., Int. Ed.* **2016**, *55*, 8381−8385. (b) Ali, A.; Barman, S. K.; Mukherjee, R. *Inorg. Chem.* **2015**, *54*, 5182−5194. (c) Comanescu, C. C.; Vyushkova, M.; Iluc, V. *Chem. Sci.* **2015**, *6*, 4570−4579. (d) Jacquet, J.; Salanouve, E.; Orio, M.; Vezin, H.; Blanchard, S.; Derat, E.; Desage-El Murr, M.; Fensterbank, L. *Chem. Commun.* **2014**, *50*, 10394−10397. (e) van der Meer, M.; Rechkemmer, Y.; Peremykin, I.; Hohloch, S.; van Slageren, J.; Sarkar, B. *Chem. Commun.* **2014**, *50*, 11104−11106. (f) Alaji, Z.; Safaei, E.; Chiang, L.; Clarke, R. M.; Mu, C.; Storr, T. *Eur. J. Inorg. Chem.* **2014**, *2014*, 6066−6074. (g) Sanz, C. A.; Ferguson, M. J.; McDonald, R.; Patrick, B. O.; Hicks, R. G. *Chem. Commun.* **2014**, *50*, 11676−11678. (h) Chang, M.-C.; Dann, T.; Day, D. P.; Lutz, M.; Wildgoose, G. G.; Otten, E. *Angew. Chem., Int. Ed.* **2014**, *53*, 4118−4122. (i) Wong, J. L.; Sánchez, R. H.; Logan, J. C.; Zarkesh, R. A.; Ziller, J.; Heyduk, A. F. *Chem. Sci.* **2013**, *4*, 1906−1910. (j) Myers, T. W.; Berben, L. A. *Chem. Commun.* **2013**, *49*, 4175−4177. (k) Ouch, K.; Mashuta, M. S.; Grapperhaus, C. A. *Inorg. Chem.* **2011**, *50*, 9904−9914. (l) Smith, A. L.; Hardcastle, K. I.; Soper, J. D. *J. Am. Chem. Soc.* **2010**, *132*, 14358−14360. (m) McKinnon, S. D. J.; Patrick, B. O.; Lever, A. B. P.; Hicks, R. G. *Chem. Commun.* **2010**, *46*, 773−775. (n) Sylvester, K. J.; Chirik, P. J. *J. Am. Chem. Soc.* **2009**, *131*, 8772−8774. (o) Königsmann, M.; Donati, N.; Stein, D.; Schönberg, H.; Harmer, J.; Sreekanth, A.; Grützmacher, H. *Angew. Chem., Int. Ed.* **2007**, *46*, 3567−3570.

(4) (a) Diao, T.; Chirik, P. J.; Roy, A. K.; Lewis, K.; Nye, S. A.; Weller, K. J.; Delis, J. G. P.; Yu, R. U.S. Patent 0080536A1, 2015. (b) Lewis, K. M.; Hojila Atienza, C. C.; Boyer, J. L.; Chirik, P. J.; Delis, J. G. P.; Roy, A. K. U.S. Patent 0330036A1, 2014. (c) Tondreau, A. M.; Chirik, P. J.; Delis, J. G. P.; Weller, K. J.; Lewis, K.; Nye, S. A. U.S. Patent 0130021A1, 2012.

(5) (a) Connor, D. M.; Keller, K. A.; Lever, J. G. U.S. Patent 0113967, 2007. (b) Sato, W.; Nakamura, T.; Takeuchi, M.; Maeda, S. Japan Patent 015181, 2007. (c) Sato, W.; Okamoto, K.; Saito, Y.; Kawashima, M.; Kaneda, T. WO 118277, 2006. (d) Saito, Y.; Sato, I.; Morii, H. Japan Patent 195399, 2006.

(6) For reviews, see ref 2a and: (a) Sarkar, B.; Schweinfurth, D.; Deibel, N.; Weisser, F. *Coord. Chem. Rev.* **2015**, *293−294*, 250−262. (b) Poddel'sky, A. I.; Cherkasov, V. K.; Abakumov, G. A. *Coord. Chem. Rev.* **2009**, *253*, 291−324. (c) Pierpont, C. G. *Coord. Chem. Rev.* **2001**, *219−221*, 415−433. (d) Pierpont, C. G. *Coord. Chem. Rev.* **2001**, *216−217*, 99−125. (e) Pierpont, C. G.; Buchanan, R. M. *Coord. Chem. Rev.* **1981**, *38*, 45−87.

(7) Selected examples: (a) Chaudhuri, P.; Verani, C. N.; Bill, E.; Bothe, E.; Weyhermüller, T.; Wieghardt, K. *J. Am. Chem. Soc.* **2001**, *123*, 2213−2223. (b) Chun, H.; Verani, C. N.; Chaudhuri, P.; Bothe, E.; Bill, E.; Weyhermüller, T.; Wieghardt, K. *Inorg. Chem.* **2001**, *40*, 4157−4166. (c) Bachler, V.; Olbrich, G.; Neese, F.; Wieghardt, K. *Inorg. Chem.* **2002**, *41*, 4179−4193. (d) Sun, X.; Chun, H.; Hildenbrand, K.; Bothe, E.; Weyhermüller, T.; Neese, F.; Wieghardt, K. *Inorg. Chem.* **2002**, *41*, 4295−4303. (e) Chun, H.; Bill, E.; Bothe, E.;

DOI: 10.1021/acs.inorgchem.6b01192
Inorg. Chem. 2016, 55, 8603−8611

Weyhermüller, T.; Wieghardt, K. *Inorg. Chem.* **2002**, *41*, 5091−5099. (f) Chun, H.; Bill, E.; Weyhermüller, T.; Wieghardt, K. *Inorg. Chem.* **2003**, *42*, 5612−5620. (g) Min, K. S.; Weyhermüller, T.; Bothe, E.; Wieghardt, K. *Inorg. Chem.* **2004**, *43*, 2922−2931. (h) Sik Min, K.; Weyhermüller, T.; Wieghardt, K. *Dalton Trans.* **2004**, 178−186.

(8) (a) Schweinfurth, D.; Rechkemmer, Y.; Hohloch, S.; Deibel, N.; Peremykin, I.; Fiedler, J.; Marx, R.; Neugebauer, P.; van Slageren, J.; Sarkar, B. *Chem.—Eur. J.* **2014**, *20*, 3475−3486. (b) Deibel, N.; Schweinfurth, D.; Hohloch, S.; Delor, M.; Towrie, M.; Sazanovich, I.; Weinstein, J.; Sarkar, B. *Inorg. Chem.* **2014**, *53*, 1021−1031. (c) Kundu, T.; Sarkar, B.; Mondal, T. K.; Mobin, S. M.; Urbanos, F. A.; Fiedler, J.; Jiménez-Aparicio, R.; Kaim, W.; Lahiri, G. K. *Inorg. Chem.* **2011**, *50*, 4753−4763. (d) Das, A. K.; Sarkar, B.; Fiedler, J.; Zalis, S.; Hartenbach, I.; Strobel, S.; Lahiri, G. K.; Kaim, W. *J. Am. Chem. Soc.* **2009**, *131*, 8895−8902. (e) Sarkar, B.; Patra, S.; Fiedler, J.; Sunoj, R. B.; Janardanan, D.; Lahiri, G. K.; Kaim, W. *J. Am. Chem. Soc.* **2008**, *130*, 3532. (f) Ghumaan, S.; Sarkar, B.; Maji, S.; Puranik, V. G.; Fiedler, J.; Urbanos, F. A.; Jiménez-Aparicio, R.; Kaim, W.; Lahiri, G. K. *Chem.—Eur. J.* **2008**, *14*, 10816−10828.

(9) (a) Hananouchi, S.; Krull, B. T.; Ziller, J. W.; Furche, F.; Heyduk, A. F. *Dalton Trans.* **2014**, *43*, 17991−18000. (b) Wong, J. L.; Sanchez, R. H.; Logan, J. G.; Zarkesh, R. A.; Ziller, J. W.; Heyduk, A. F. *Chem. Sci.* **2013**, *4*, 1906−1910. (c) Szigethy, G.; Heyduk, A. F. *Dalton Trans.* **2012**, *41*, 8144−8152. (d) Blackmore, K. J.; Sly, M. B.; Haneline, M. R.; Ziller, J. W.; Heyduk, A. F. *Inorg. Chem.* **2008**, *47*, 10522−10532. (e) Blackmore, K. J.; Ziller, J. W.; Heyduk, A. F. *Inorg. Chem.* **2008**, *47*, 265−273. (f) Zarkesh, R. A.; Ziller, J. W.; Heyduk, A. F. *Angew. Chem., Int. Ed.* **2008**, *47*, 4715−4718.

(10) (a) Shekar, S.; Brown, S. N. *Dalton Trans.* **2014**, *43*, 3601−3611. (b) Rajput, A.; Sharma, A. K.; Barman, S. K.; Koley, D.; Steinert, M.; Mukherjee, R. *Inorg. Chem.* **2014**, *53*, 36−48. (c) Cipressi, J.; Brown, S. N. *Chem. Commun.* **2014**, *50*, 7956−7959. (d) Ghisolfi, A.; Waldvogel, A.; Routaboul, L.; Braunstein, P. *Inorg. Chem.* **2014**, *53*, 5515−5526. (e) Banerjee, S.; Halder, P.; Paine, T. K. *Z. Anorg. Allg. Chem.* **2014**, *640*, 1168−1176. (f) Randolph, A. H.; Seewald, N. J.; Rickert, K.; Brown, S. N. *Inorg. Chem.* **2013**, *52*, 12587−12598. (g) Shekar, S.; Brown, S. N. *Organometallics* **2013**, *32*, 556−564. (h) Ringenberg, M. R.; Kokatam, S. L.; Heiden, Z. M.; Rauchfuss, T. B. *J. Am. Chem. Soc.* **2008**, *130*, 788−789. (i) Dei, A.; Gatteschi, D.; Pardi, L. *Inorg. Chem.* **1990**, *29*, 1442−1444.

(11) (a) Brown, S. N. *Inorg. Chem.* **2012**, *51*, 1251−1260. See also: (b) Bhattacharya, S.; Gupta, P.; Basuli, F.; Pierpont, C. G. *Inorg. Chem.* **2002**, *41*, 5810−5816.

(12) Fe(II): (a) King, E. R.; Hennessy, E. T.; Betley, T. A. *J. Am. Chem. Soc.* **2011**, *133*, 4917−4923. (b) Hennessy, E. T.; Betley, T. A. *Science* **2013**, *340*, 591−595. (c) Hennessy, E. T.; Liu, R. Y.; Iovan, D. A.; Duncan, R. A.; Betley, T. A. *Chem. Sci.* **2014**, *5*, 1526−1532. (d) Iovan, D.; Betley, T. A. *J. Am. Chem. Soc.* **2016**, *138*, 1983−1993. (e) Thacker, N. C.; Lin, Z.; Zhang, T.; Gilhula, J. C.; Abney, C. W.; Lin, W. *J. Am. Chem. Soc.* **2016**, *138*, 3501−3509.

(13) Co(II): (a) Cui, X.; Xu, X.; Jin, L.-M.; Wojtas, L.; Zhang, X. P. *Chem. Sci.* **2015**, *6*, 1219−1224. (b) Goswami, M.; Lyaskovskyy, V.; Domingos, S. R.; Buma, W. J.; Woutersen, S.; Troeppner, O.; Ivanović-Burmazović, I.; Lu, H.; Cui, X.; Zhang, X. P.; Reijerse, E. J.; DeBeer, S.; van Schooneveld, M. M.; Pfaff, F. F.; Ray, K.; de Bruin, B. *J. Am. Chem. Soc.* **2015**, *137*, 5468−5479. (c) Lu, H.-J.; Li, C.-Q.; Jiang, H.-L.; Lizardi, C. L.; Zhang, X. P. *Angew. Chem., Int. Ed.* **2014**, *53*, 7028−7032. (d) Paul, N. D.; Mandal, S.; Otte, M.; Cui, X.; Zhang, X. P.; de Bruin, B. *J. Am. Chem. Soc.* **2014**, *136*, 1090−1096. (e) Otte, M.; Kuijpers, P. F.; Troeppner, O.; Ivanović-Burmazović, I.; Reek, J. N. H.; de Bruin, B. *Chem.—Eur. J.* **2014**, *20*, 4880−4884. (f) Ruppel, J. V.; Cui, X.; Xu, X.; Zhang, X. P. *Org. Chem. Front.* **2014**, *1*, 515−520. (g) Jin, L.-M.; Lu, H.-J.; Cui, Y.; Lizardi, C. L.; Arzua, T. N.; Wojtas, L.; Cui, X.; Zhang, X. P. *Chem. Sci.* **2014**, *5*, 2422−2427.

(14) Rh(0): Puschmann, F. F.; Grützmacher, H.; de Bruin, B. *J. Am. Chem. Soc.* **2010**, *132*, 73−75.

(15) Rh(II): (a) To, C. T.; Choi, K. S.; Chan, K. S. *J. Am. Chem. Soc.* **2012**, *134*, 11388−11391. (b) Chan, Y. W.; Chan, K. S. *J. Am. Chem. Soc.* **2010**, *132*, 6920−6922. (c) Chan, K.-S; Li, X. Z.; Dzik, W. I.; de Bruin, B. *J. Am. Chem. Soc.* **2008**, *130*, 2051−2061. (d) Hetterscheid, D. G. H.; Klop, M.; Kicken, R. J. N. A. M; Smits, J. M. M.; Reijerse, E. J.; de Bruin, B. *Chem.—Eur. J.* **2007**, *13*, 3386−3405. See also: (e) Wayland, B. B.; Poszmik, G.; Fryd, M. *Organometallics* **1992**, *11*, 3534−3542.

(16) Ir(II): (a) Hetterscheid, D. G. H.; Kaiser, J.; Reijerse, E.; Peters, T. P. J.; Thewissen, S.; Blok, A. N. J.; Smits, J. M. M.; de Gelder, R.; de Bruin, B. *J. Am. Chem. Soc.* **2005**, *127*, 1895−1905. (b) Hetterscheid, D. G. H.; Bens, M.; de Bruin, B. *Dalton Trans.* **2005**, *5*, 979−984. (c) de Bruin, B.; Thewissen, S.; Yuen, T.-W.; Peters, T. P. J.; Smits, J. M. M.; Gal, A. W. *Organometallics* **2002**, *21*, 4312−4314. (d) de Bruin, B.; Peters, T. P. J.; Thewissen, S.; Blok, A. N. J.; Wilting, J. B. M.; de Gelder, R.; Smits, J. M. M.; Gal, A. W. *Angew. Chem., Int. Ed.* **2002**, *41*, 2135−2138.

(17) (a) Sengupta, D.; Saha Chowdhury, N.; Samanta, S.; Ghosh, P.; Seth, S. K.; Demeshko, S.; Meyer, F.; Goswami, S. *Inorg. Chem.* **2015**, *54*, 11465−11476. (b) Broere, D. L. J.; Metz, L. L.; de Bruin, B.; Reek, J. N. H.; Siegler, M. A.; van der Vlugt, J. I. *Angew. Chem., Int. Ed.* **2015**, *54*, 1516−1520. (c) Zhou, W.; Patrick, B. O.; Smith, K. M. *Chem. Commun.* **2014**, *50*, 9958−9960. (d) Lippert, C. A.; Arnstein, S. A.; Sherrill, C. D.; Soper, J. D. *J. Am. Chem. Soc.* **2010**, *132*, 3879−3892.

(18) (a) Broere, D. L. J.; de Bruin, B.; Reek, J. N. H.; Lutz, M.; Dechert, S.; van der Vlugt, J. I. *J. Am. Chem. Soc.* **2014**, *136*, 11574−11577. For related Pd(**NNO**) chemistry, see: (b) Broere, D. L. J.; Demeshko, S.; de Bruin, B.; Pidko, E. A.; Reek, J. N. H.; Siegler, M. A.; Lutz, M.; van der Vlugt, J. I. *Chem.—Eur. J.* **2015**, *21*, 5879−5886. (c) Broere, D. L. J.; Plessius, R.; Tory, J.; Demeshko, S.; de Bruin, B.; Siegler, M. A.; Hartl, F.; van der Vlugt, J. I. *Chem.—Eur. J.* **2016**, *22*, YYY DOI: 10.1002/chem.201601900.

(19) These values are slightly different than those previously reported (ref 18a), because of incorrect previous referencing of the Fc/Fc^+ couple.

(20) The reason behind the observed spectral broadening remains unclear, but it may be related to fluxional coordination behavior of the $\mathbf{NNO}^{\mathbf{IBQ}}$ ligand. Alternatively, workup and spectroscopy under ambient conditions in the absence of excess oxidant may result in partial regeneration of **1**, leading to broadened spectral features (due to a self-exchange process or the presence of a paramagnetic species).

(21) Kokatam, S.; Weyhermüller, T.; Bothe, E.; Chaudhuri, P.; Wieghardt, K. *Inorg. Chem.* **2005**, *44*, 3709−3717.

(22) Although there is no single resonance structure that fully captures the electronic structure in **1**, the resonance structure that is commonly depicted for these systems, with a radical on C1 (bound to oxygen), appears to be most suitable for complex **1**. The spin density for complex **1** is localized to a significant extent on the iminosemiquinonato nitrogen,[18] which would support the alternative representation of an aromatic phenyl ring with an aminyl radical. However, the significant dearomatization observed in the molecular structure of $PdCl(\mathbf{NNO}^{\mathbf{ISQ}})$ shows that this is a poor description of the actual situation. A description with the radical located on C6 accurately reflects the observed dearomatization but does not correspond with the localization of spin density.

(23) (a) Ali, A.; Barman, S. K.; Mukherjee, R. *Inorg. Chem.* **2015**, *54*, 5182−5194. For a related series of Pd(II) with a redox-active ligand in three oxidation states, see: (b) Gautam, R.; Loughrey, J. J.; Astashkin, A. V.; Shearer, J.; Tomat, E. *Angew. Chem., Int. Ed.* **2015**, *54*, 14894−14897.

(24) Kokatam, S.; Chaudhuri, P.; Weyhermüller, T.; Wieghardt, K. *Dalton Trans.* **2007**, 373−378.

(25) Warratz, R.; Peters, G.; Studt, F.; Römer, R.-H.; Tuczek, F. *Inorg. Chem.* **2006**, *45*, 2531−2542.

(26) Nielson, R. M.; McManis, G. E.; Golovin, M. N.; Weaver, M. J. *J. Phys. Chem.* **1988**, *92*, 3441−3450.

(27) This observation may explain why no (volatile) 1,2-dichloroethane was observed by gas chromatography and mass spectrometry or NMR. Other possible reaction pathways for decomposition of the chloromethyl radical, including disproportionation reactions, were not considered for DFT calculations. We have not attempted the reaction of **2** with other chlorinated reagents.

DOI: 10.1021/acs.inorgchem.6b01192
Inorg. Chem. 2016, 55, 8603−8611

(28) For the corresponding gas phase calculations, see the Supporting Information.
(29) Using the pure GGA BP86 functional provided similar results.
(30) The applied broken symmetry approach is an approximation of the multideterminant problem of bond-splitting reactions, hence introducing some (unavoidable) additional error into the computed barrier.
(31) Emmi, S. S.; Beggiato, G.; Casalbore-Miceli, G. *Int. J. Radiat. Appl. Instrum. C Radiat. Phys. Chem.* **1989**, *33*, 29−37.
(32) Most likely resulting from catalyst decomposition. This compound is also the main product at higher reaction temperatures. Nitrile **6** is thus an unlikely source of H atoms to generate linear amine **5**.
(33) Reaction with benzyl bromide appears to be very facile. For a related study, see: Broere, D. L. J.; Modder, D. K.; Blokker, E.; Siegler, M. A.; van der Vlugt, J. I. *Angew. Chem., Int. Ed.* **2016**, *55*, 2406−2410.
(34) Connelly, N. G.; Geiger, W. E. *Chem. Rev.* **1996**, *96*, 877−910.
(35) Drouet, F.; Fontaine, P.; Masson, G.; Zhu, J. *Synthesis* **2009**, *2009*, 1370−1374.
(36) *APEX2*; Bruker: Madison, WI, 2014.
(37) Sheldrick, G. M. *SADABS*; Universität Göttingen: Göttingen, Germany, 2008.
(38) Sheldrick, G. M. *SHELXL2013*; University of Göttingen: Göttingen, Germany, 2013.
(39) Spek, A. L. *Acta Crystallogr., Sect. D: Biol. Crystallogr.* **2009**, *65*, 148−155.
(40) Ahlrichs, R. *Turbomole*, version 6.5; Theoretical Chemistry Group, University of Karlsruhe: Karlsruhe, Germany, 2002.
(41) *PQS*, version 2.4; Parallel Quantum Solutions: Fayetteville, AR, 2001. The Baker optimizer (see Baker, J. *J. Comput. Chem.* **1986**, *7*, 385−395) is available separately from Parallel Quantum Solutions upon request.
(42) Budzelaar, P. H. M. *J. Comput. Chem.* **2007**, *28*, 2226−2236.
(43) Yamanaka, S.; Kawakami, T.; Nagao, H.; Yamaguchi, Y. *Chem. Phys. Lett.* **1994**, *231*, 25−33.

DOI: 10.1021/acs.inorgchem.6b01192
Inorg. Chem. 2016, 55, 8603−8611